Article

Alternative Solution for Towing Systems Used in the Automotive Industry

Andrei Victor Petrici [1], Maria Luminita Scutaru [1,*], Vasile Gheorghe [1] and Sorin Vlase [1,2]

[1] Department of Mechanical Engineering, Faculty of Mechanical Engineering, Transylvania University of Brasov, B-dul Eroilor 29, 500036 Brasov, Romania; petrici.andrei.victor@unitbv.ro (A.V.P.); ghesile@yahoo.com (V.G.); svlase@unitbv.ro (S.V.)

[2] Technical Sciences Academy of Romania, B-dul Dacia 26, 030167 Bucharest, Romania

* Correspondence: lscutaru@unitbv.ro

Featured Application: Towing systems are largely used in the automotive industry. They must respect some requirements defined by the standards. These important systems for cars are studied in this paper in order to improve safety in transportation. The authors present the possibility to use other materials for towbars and formulate a series of practical recommendations obtained as a result of extended studies on towing systems.

Abstract: This paper aims, in the context of the need to reduce the weight and price of vehicles, to present theoretical and experimental results regarding towing systems made of alternative materials (fibrous composite materials and aluminum alloys). The study of the main element of the whole system, namely towbar research, was stressed, presenting comparative results. The FEM will be used to obtain the stress and strain field in the towball and the towing system. The experimental tests validate the theoretical results obtained. This paper studies five towing systems made by different materials and finally presents a series of practical recommendations, useful in the industry, regarding the improvement of the analyzed models.

Keywords: towing system; stress; strain; safety; car; finite element method

1. Introduction

The growing need to transport objects and people with the same vehicle led to the emergence of the trailer. The trailer is a vehicle that does not have the ability to propel itself, needing another towing vehicle to move it. Currently, the shapes of trailers are very varied and are used in countless fields of transport. In automotive engineering, trailers and semi-trailers for cars have a lot of destinations, not just to transport goods or people. The roles assigned to the most common trailers are as follows: caravan, platform with tarpaulin, without tarpaulin, electric current generator, tanker, tipper, concrete mixer, refrigerated transport, store, nacelle, animal transport, etc. Semi-trailers are trailers that lack the front axle; during operation, they rest on the rear of the vehicle. For cars, the most common are semi-trailers, the two-axle trailer being most often found on platforms or where the weight is high; it requires balance when stationary and/or this is required for various reasons. Due to the regime during the operation of the car–trailer assembly, the coupling between these two vehicles must be very resistant, both to dynamic and static loads, but also to the influence of chemical and meteorological factors.

The connection between the vehicle and the towed vehicle is made with a complex towing system; among the most important components of this system is the towing hook (towball or towbar). Towing systems for cars are completely different from other systems found in trucks, tractors, etc. In general, car towing systems are similar in shape, but different dimensionally from car to car, due to body shape, gauge, vehicle height and other reasons, which also differ from car model to car model.

Most tow hooks are made of a circular bar that is turned and then bent, flattened and drilled, which is also the order of operations in the technological itinerary. The standard of the towing hook requires the ball to have a diameter of 50 mm; the construction of the trailer is thus made with a coupler whose inner radius is made in such a way as to allow the penetration and rotation of the ball of the hook.

The towing industry has recently seen a great deal of diversification. First of all, this is due to the appearance of new material, but also due to the improvement in the means of calculation and testing. Thus, there is a continuous increase in the use of composite materials in this field. Recently, car manufacturers have introduced composite materials and aluminum alloys both in the composition of the body and chassis, as well as in the composition of the engine parts, in order to reduce masses and increase the performance of the engines, which is why the implementation of composites and alloys in the towing assembly is referred to in [1]. Another important benefit of the use of alternative materials is that, having lower masses than those of classic materials [2], they contribute to reducing the level of noxes produced by the thermal engine of vehicles. General issues raised by the use of composite materials can be found in [3–5]. A presentation of the problems related to the use of other materials in the towing system is given in [6].

Experimental methods have also helped in the development of the field. Two such studies present vehicle engineering problems related to the towing system [7,8]. Thanks to new materials and advanced testing procedures, the design of these systems has been improved. Thus, these procedures can be applied in the design of specific towing systems [9–11]. In the last few years, a number of papers have been dedicated to the study of towing systems [12–18].

The finite element method (FEM) in its classic form [19] has proved to be an extremely powerful tool for the development of research in the field of engineering vehicles and their components [20]. A study dedicated to towing systems in parallel using the FEM is presented in [21]. Different aspects related to the study, design, and manufacturing of these systems can be found in [22–29].

One study analyzed the effects of different natures, which the replacement of a classic material for a towbar with new, cheaper and easy-to-manufacture materials generates in the practice of automobile manufacturing [30–34]. A series of relatively recent results regarding towing systems and the materials used are presented in [35–44].

The theoretical results are obtained with a finite element model. Thus, the deformations and stress that appear in the system made of different materials are determined. The obtained results are validated by experimental measurements. The research carried out allows the formulation of conclusions and recommendations regarding the use of alternative materials in the manufacture of towing systems. More and more, the problem is environmental pollution. The use of classical steel is safe and very well known in various engineering applications, and steel has a low price compared to other materials. Conversely, the big disadvantage of steel is mass/specific gravity. This leads to a higher weight of the entire vehicle, which means more pollution. On the other hand, the replacement of classic materials with lighter materials contributes to increasing the performance of the cars. By carrying components with lower masses, they consume less fuel and have better acceleration times. In conclusion, the novelty brought by this work consists of the introduction of composite materials and aluminum in the manufacture of the towbar [45–50]. These materials have properties similar to those of steel and bring cost and recycling benefits.

2. Models and Methods

2.1. Presentation of the Studied Towing System

The connection between the motor vehicle and the towed vehicle is made with a complex towing system; among the most important components of this system is the towing hook. Due to the regime during the operation of the car–trailer assembly, the coupling between these two vehicles must be very resistant, both to dynamic and static loads, but also to the influence of chemical and meteorological factors.

The general shape of the towing system is shown in Figure 1, with the same components found in all passenger car systems, but with different shapes. The composition of the towing systems is approximately the same for all car models. The towing hook can have many shapes, so as not to overlap the rear bumper of the car but also depending on the model of the hook.
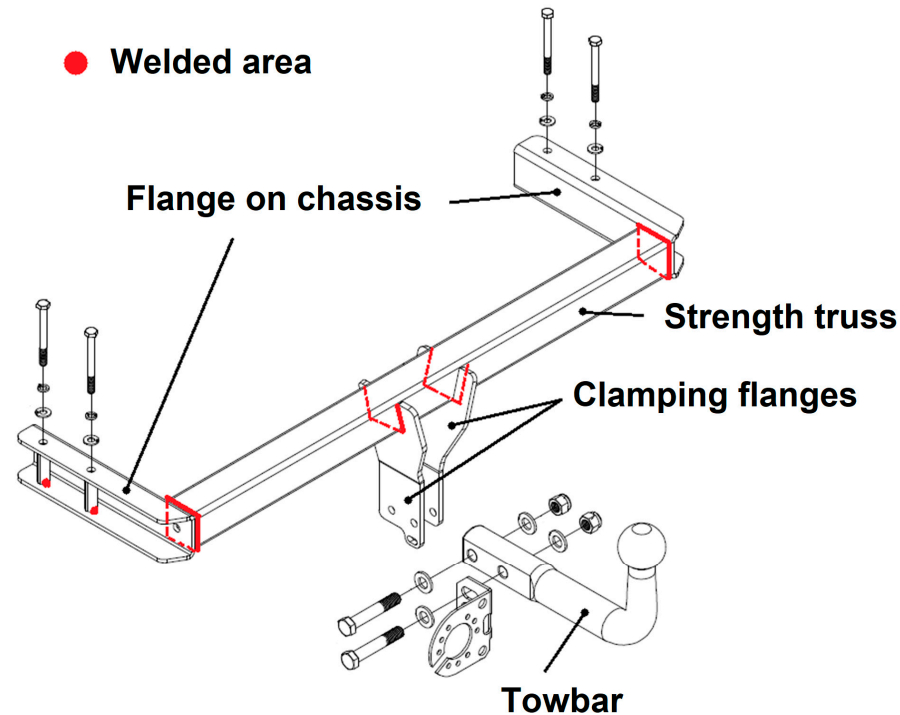
● Welded area

Flange on chassis

Strength truss

Clamping flanges

Towbar

Figure 1. The structure of the towing system used in cars.

The most common towing hooks used in cars are L-shaped ones (Figure 2). The dimensioning of a hook is carried out taking into account the load it must support, but it must also take into account the rear bumper that it must bypass, so that the length L is considered to be the distance between the center of the sphere and the middle of the distance between the two holes, and the height H is the distance between the center of the sphere and the axis passing between the two holes (Figure 2). The diameter of the hook sphere is set by the standards at 50 mm.
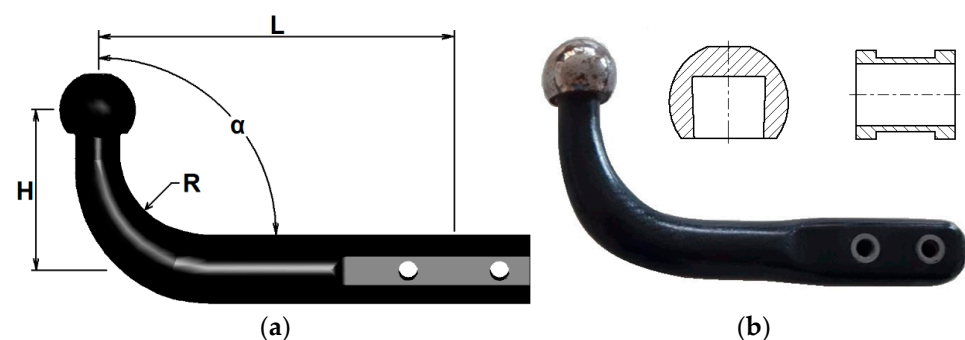
(a) **(b)**

Figure 2. L-shaped towing hook. **(a)** Made by steel; **(b)** made by carbon fiber.

The towing system chosen to carry out the theoretical and experimental research is equipped with a simple towing hook, fixed with two screws to the central flanges on the resistance beam. The dimensions, necessary for this study, of the towing system for which mechanical resistance calculations are performed are shown in Figure 3.
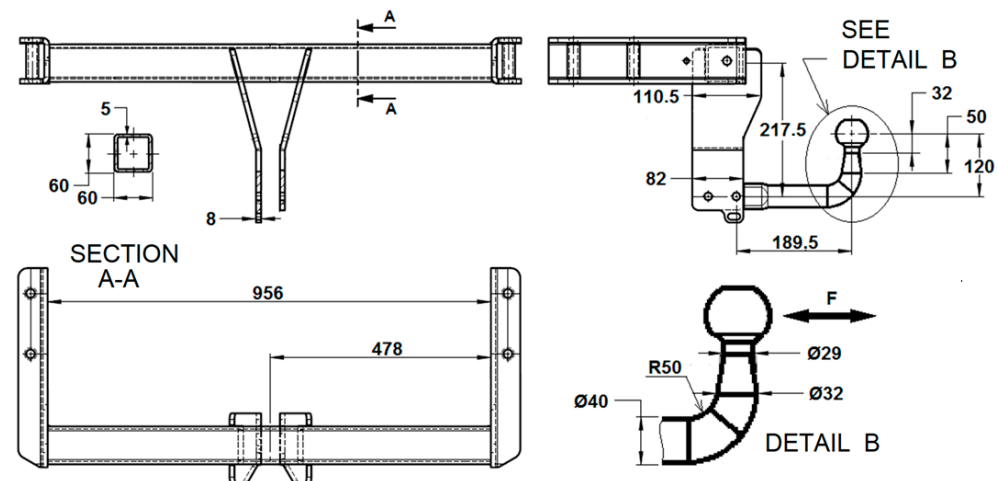
Figure 3. Dimensions of the towing system.

Since several specific areas of the towbar will be mentioned, a division is proposed in Figure 4 that will facilitate its presentation.
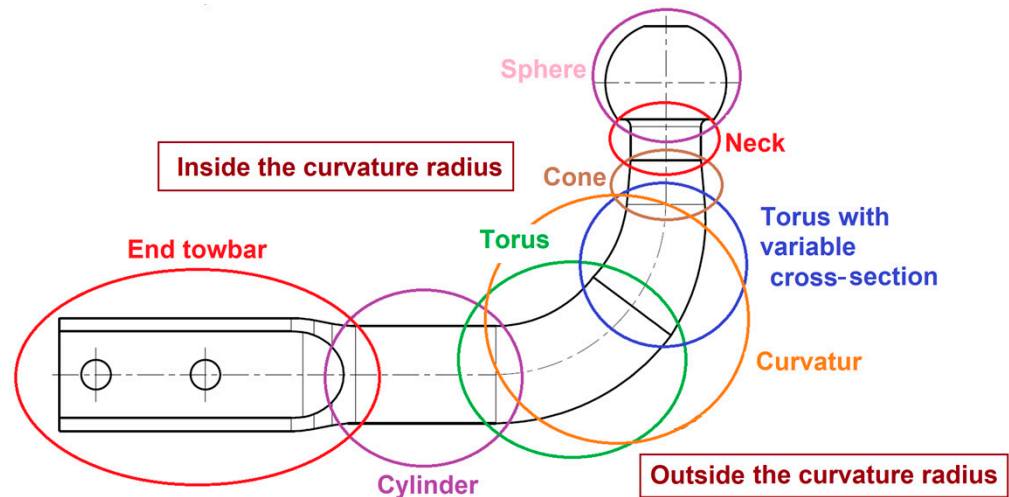

Figure 4. Towing hook areas.

2.2. Materials Used for the Manufacture of the Towball

1. Steel hook. It is the solution adopted everywhere at the moment, the steel being easy to obtain, being easy to process and having very good mechanical properties. Some disadvantages will be mentioned next. For steel, the properties considered in the paper are as follows: $E = 2.1 \cdot 10^5$ [N/mm^2], $\sigma_e = 355$ [N/mm^2] and $\sigma_r = 470 \div 630$ [N/mm^2].

2. Carbon fiber towbar (Figure 2b). It is one of the solutions we propose in this paper. It will be described in detail below (see properties in [35]). For the benefit of mechanical properties, the carbon fibers in the structure of the towbar are continuous.

3. Aluminum and aluminum alloys. Aluminum alloys with silicon have the advantage of being easily obtained by casting. Also, the mechanical properties of siluminum are very high, which is why they are very common in applications where resistance to mechanical shocks and fatigue is required. The multiple advantages offered by silumins have increased interest in making the towing hook from this material. Additionally, to highlight the major differences in mechanical testing between pure aluminum and aluminum, it was decided to make the towing hook including 99.7% aluminum.

Since by comparing the tensile and bending results of the specimens from the two types of alloys, AlSi10MnMg and AlSi12Cu1Fe, different behaviors in terms of strength

were observed, it was decided to make the towing hook from both AlSi10MnMg and AlSi12Cu1Fe, two materials found in the automotive industry. The process of obtaining the aluminum towbar is by manual gravity casting [36–40] (see Figure 5).

Figure 5. Towing hook obtained by gravity casting.

The raw semi-finished product obtained by gravity casting must be mechanically processed to obtain a towing hook made of aluminum or silumin. During the research, six towing hooks were studied, three obtained by the gravity casting process from aluminum with a purity of 99.7% and aluminum alloy (AlSi10MnMg and AlSi12Cu1Fe) and then through the related mechanical processing. To these are added the steel and carbon fiber towing hooks, thus resulting in 5 types of hooks made of different materials, namely the following:

1.   Steel (S355J2);
2.   Carbon fibers;
3.   Al99.7% (pure aluminum);
4.   AlSi10MnMg;
5.   AlSi12Cu1Fe.

2.3. Finite Element Method (FEM)

2.3.1. Modeling the Towing System

The studied towing system is made up of several components, as shown in Figure 6, the constituent elements also being shown in the figure.
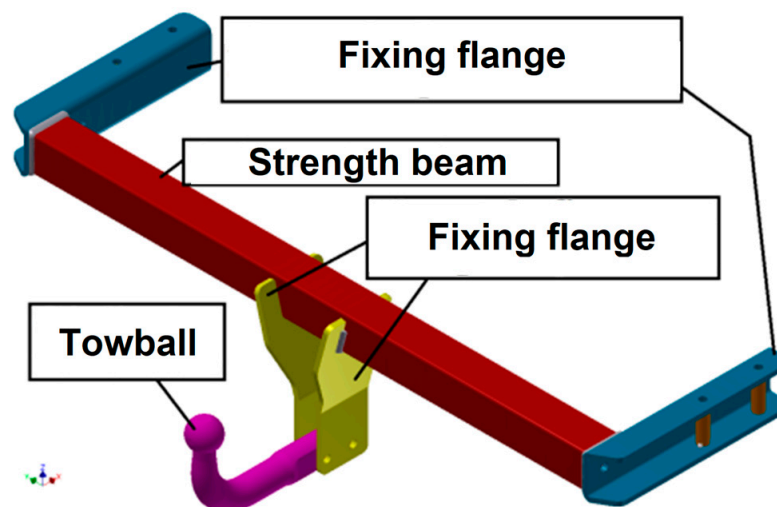

Figure 6. Modeling of the towing system.

Figure 7 show the views from the side of the vehicle and from above it, respectively, where the direction of force action can be observed.

Figure 7. Views of the assembly. (**a**) Side view; (**b**) top view.

The towing system modeling in this paper is carried out in the Inventor software 2020 developed by the AutoDesk company (San Francisco, CA, USA), and the FEM simulation is carried out with the same software. Each constituent element of the towing system is analyzed individually, after which the entire assembly is studied. The areas of interest for determining the stresses are at the two ends of the beam and the radius of curvature of the tow hook, inside. Therefore, the results obtained from FEM simulations in these areas will be emphasized.

2.3.2. Model Discretization and Finite Element Analysis

The resistance beam and the flanges welded to it have simple geometry, which can be represented via discretization by 2D surfaces or even 1D lines in the case of the beam and outer flanges. Instead, the geometry of the tow hook is variable along its entire length, making it inefficient to discretize this model into lines or surfaces. Therefore, the discretization of the entire towing system is carried out with 3D volume elements, an advantageous variant both for satisfying the requirement given by the geometry of the hook and, visually, for interpreting the method of deformation of the entire towing subassembly. Following the classical calculations, it is observed that the most loaded component in the structure of the towing system is the hook. As a consequence, two analyses are carried out in parallel, both of the entire towing system and, on a specific basis, only of the towing hook.

Figure 8 shows the discretization of the entire towing system, the discretization consisting of 41,347 elements and 73,004 nodes.
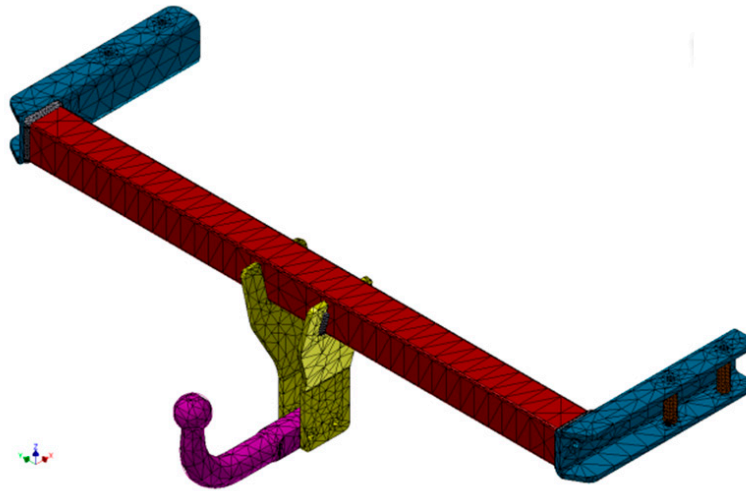
Figure 8. Discretization of the towing system.

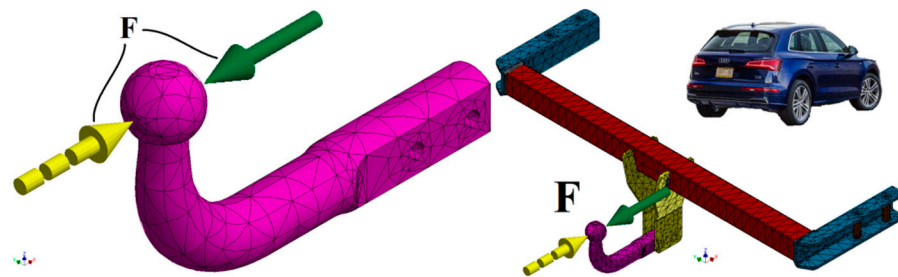Figure 9 shows the discretization of the tow hook, a discretization composed of 3827 nodes and 2262 elements.

Figure 9. Discretization of the towing hook and direction of force in the hook and in the towing system.

Force is applied in the center of the sphere, in the longitudinal direction of the vehicle, in the direction towards the car, and the value of the force acting on the towing system is $F = 7.5$ kN, see Figure 9.

The chosen material has the properties necessary for the calculation of stresses and displacements similar to those of the steel used to make the towing assembly.

2.3.3. Extracting the Target Results from the Software

From the interpretation of the classical resistance calculation of the towing system, it is found that the areas of interest for FEM analysis are in the inner bending area of the towing hook, but also the outer ends of the towing beam, which is why the analysis will focus on these places.

Looking at the deformations in the studied system, the arrow from the towing hook to the sphere is of interest as the geometry that undergoes the greatest displacement. The welded flanges on the resistance beam have generous sections, which is why insignificant forces were observed in the classical calculation; therefore, the deformations necessary to determine the displacements are insignificant.

2.3.4. Stresses in System

Shown in Figure 10 is the overview of the towing system, highlighting in multi-color the stressed areas after applying the force to the system, according to the color legend on the left side of the image of the simulation software.
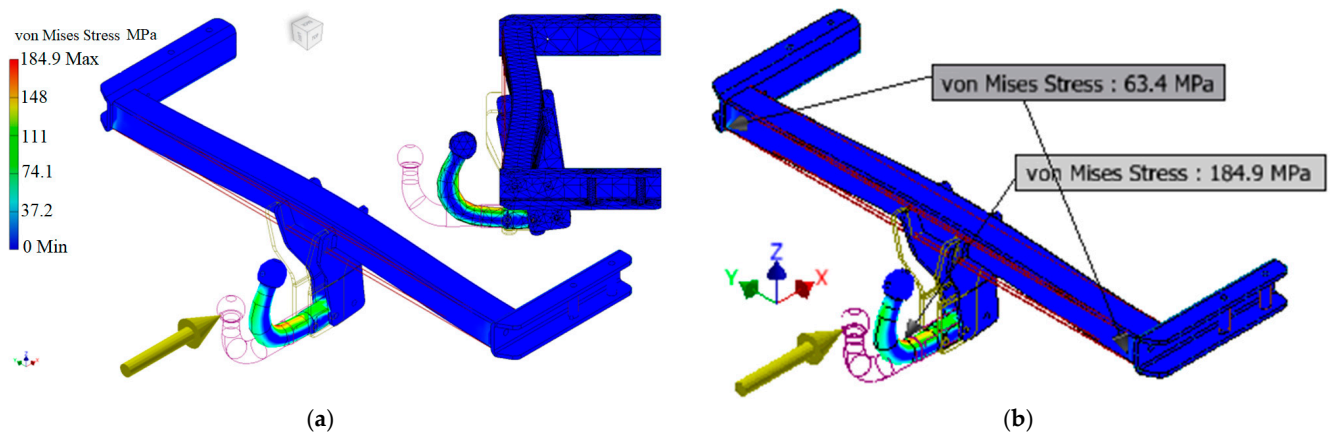
(**a**)   (**b**)

Figure 10. (**a**) Deformation mode and (**b**) von Mises stresses appearing in the towing hook and strength beam.

It can be seen how the highest stress appears in the hook, and the points of interest appear in the area of the ends of the beam, but they are not as stressed as those in the towing hook. Analyzing the deformation mode of the system, slight torsion of the beam is observed, thus justifying the classic torsional calculation of this component.

The equivalent stresses appearing in the two elements of interest of the towing system are shown in Figure 10.

It is observed that the maximum stress that occurs in the beam is not exactly at the ends. Being a symmetrically stressed bar, embedded at both ends, the highest stress occurs slightly away from the embedded area, and in this case the points of maximum stress occur 8.2 mm from the ends.

Going into the detailing of the towing hook, the most stressed component in the system, it is observed that the inner part experiences higher stresses than the outer part.

The maximum stress developed in the towing hook and the stress developed in the outer bending area are shown in Figure 11, but the deformation is exaggerated to understand the extreme mode of deformation, where very high unforeseen forces may occur.
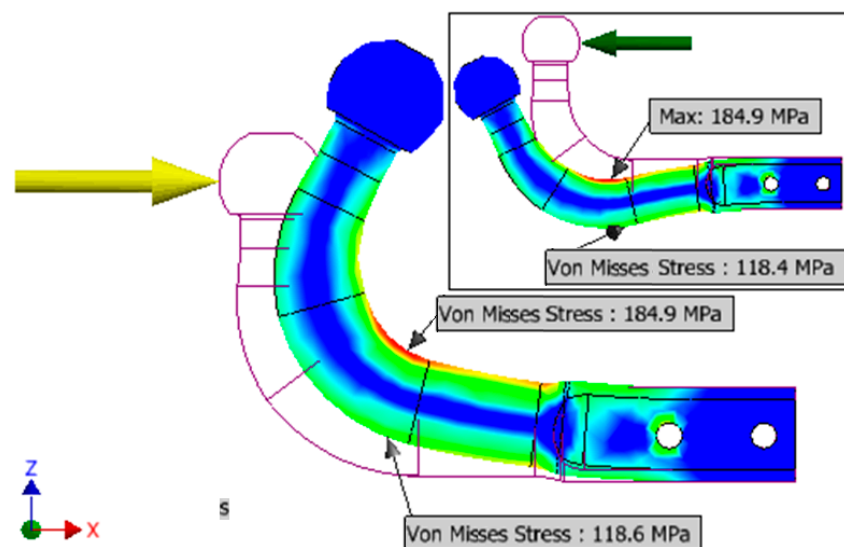

Figure 11. Von Mises stresses appearing in the towing hook.

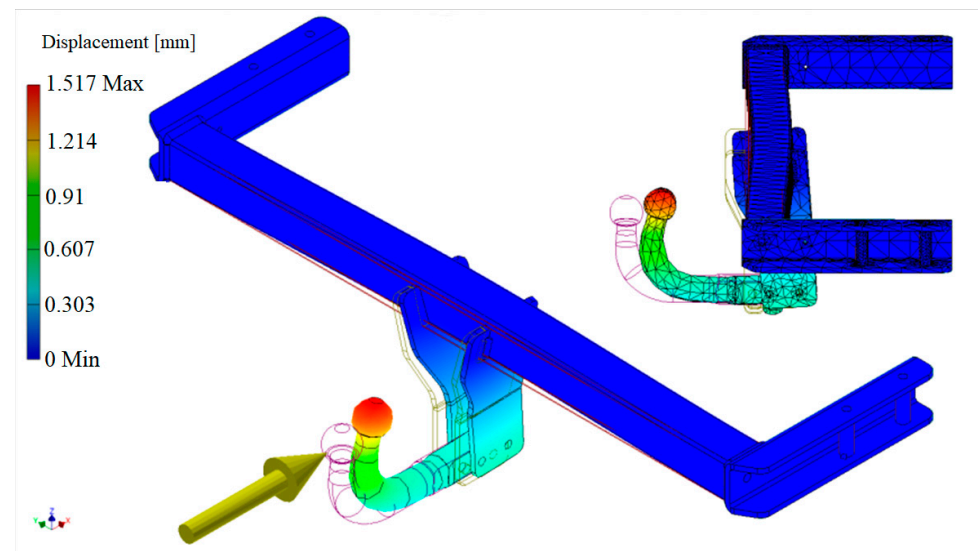In Table 1, the stresses arising in the towing system are centralized.

Table 1. Centralization of the specific values of stresses in the system.

The Requested Component	The Area of the Resulting Stress	Stress [MPa]
The inside of the radius of curvature	The inside of the radius of curvature, σ_{int}	184.9
	The outside of the radius of curvature, σ_{ext}	118.6
Resistance beam	Extremity	63.4

2.3.5. Determination of Displacements

In terms of displacements, the major interest is in determining the displacement given by the sphere of the towing hook in the horizontal plane, towards the car, so that there is no risk of coming into contact with its bumper.

Figure 12 shows the overview of the towing system, highlighting the areas that experience the most pronounced displacements after force is applied to the system, according to the legend.

Figure 12. Displacements and (exaggerated) deformation mode of the towing system.

Analyzing the deformation mode of the towing system, three important aspects are found (see Figure 13) that express the initial state and the deformed state of the system, namely the following:

- The maximum displacement occurs at the top left point of the flattening on the hook sphere. The point marked with '2' in Figure 13 represents the place where the most pronounced displacement of the towing system takes place—this point is of less interest in the displacements in the system. The point marked with '1' in the same figure represents the specific point of the center of the sphere, its displacement making the object of interest.
- The sphere moves in two directions. Looking at the studied system from the side of the car (Figure 13), it can be seen that the sphere moves both in the direction X+ (horizontally towards the vehicle) and in the direction Z+ (vertically towards the roof of the car), creating a compound movement. The values of the displacements u_1, v_1, u_2 and v_2, but also their vector compounds δ_{u1-v1} and δ_{u2-v2}, are specified in Table 2.
- The torsion of the beam tends to cancel out the displacement of the sphere. It can be seen in Figure 13 that the deformation of the hook is achieved by bending in the clockwise direction, and the deformation of the beam is achieved in the opposite

direction of rotation (along with the entire towing hook). Therefore, this composition of displacements tends to return the hook sphere to its original position. The return to the initial state of the ball is not achieved because the displacement from the bending of the hook is more pronounced than the reverse displacement given by the torsion of the beam; therefore, the ball tends to move towards the vehicle.
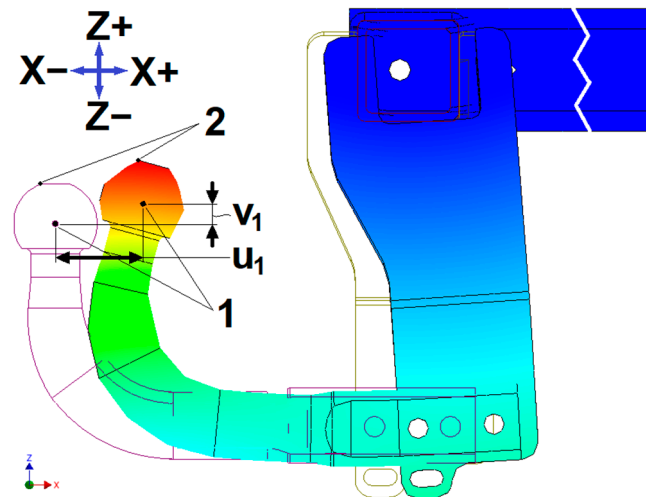

Figure 13. Aspects regarding the movements of the towing system.

Table 2. Centralization of the specific values of the displacements in the system, considering the entire towing system.

Displacement	Symbol	Value [mm]
The horizontal displacement of the center of the sphere	u_1	1.313
Vertical displacement of the center of the sphere	v_1	0.295
Compound displacement of the center of the sphere	$\delta_{u1\text{-}v1}$	1.346
Maximum horizontal displacement of the sphere	$u_{max} = u_2$	1.474
Maximum vertical displacement of the sphere	$v_{max} = v_1$	0.357
Maximum compound displacement of the sphere	$\delta_{max} = \delta_{u1\text{-}v1}$	1.517

The displacement value u_1 represents an object of interest of this paper.

Regarding deformation of the towing hook, in Table 3 the specific displacement of the center of the sphere horizontally u_1' and vertically v_1', respectively, is observed. Figure 14 shows the displacement of the single towing hook, considering it embedded in the area of the fixing holes.

Table 3. The values of the displacements in the system, considering only the individual towing hook.

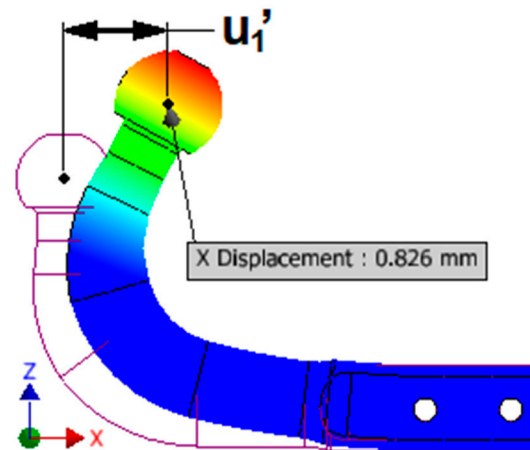| Displacement	Symbol	Value [mm]
Horizontal displacement of the center of the sphere	u_1'	0.826
Vertical displacement of the center of the sphere	v_1'	0.589
Compound displacement of the center of the sphere	$\delta_{u1'\text{-}v1'}$	1.015

Figure 14. Aspects regarding towing hook movements.

Comparing the vector displacement in the two directions of the individual hook sphere (Figure 14) and of the hook sphere in the towing assembly (Figure 13) shows a difference. The ratio of horizontal to vertical displacement is higher for a single hook, indicating that beam torsion tends to reduce the vertical displacement of the sphere more or less over the horizontal.

The displacement value u_1' represents an object of interest of this paper.

Two cases were analyzed: on the one hand, the study of the entire towing assembly; on the other hand, the study of the individual towing hook, the component that is the most important in the system.

The structure of the towing assembly is considered embedded in its outer flanges, after which a force of 7.5 kN acts in the center of the sphere of the towing hook, in a horizontal direction, towards the vehicle, simulating the braking of the assembly consisting of the vehicle and the trailer.

3. Experimental Results

3.1. Detailing the Experimental Process

We mention the following:

- The experimental determinations consist of testing, on the one hand, the entire towing system and, on the other hand, the towing hooks on a traction machine, simulating vehicle braking with a trailer, an application transposed into compression on the traction machine. The state-of-the-art traction machine has a force capacity of 100 tons and accuracy convenient for experiments (MTS).
- The target of the experimental determinations is that the samples of the tow hooks withstand a force greater than or at least equal to 7500 N, this value resulting from the calculation of heavy braking of a motor vehicle with an attached trailer, where the trailer tends to push the motor vehicle forward.

Towing hooks manufactured from various types of materials were tested, each towing hook being tested individually.

3.2. Experimental Tests on the Towing System

The towing assembly is (Figure 15) a structure with complex geometry subjected to stress, in which stress and strain cannot be easily identified and measured, requiring several sets of previously performed calculations.
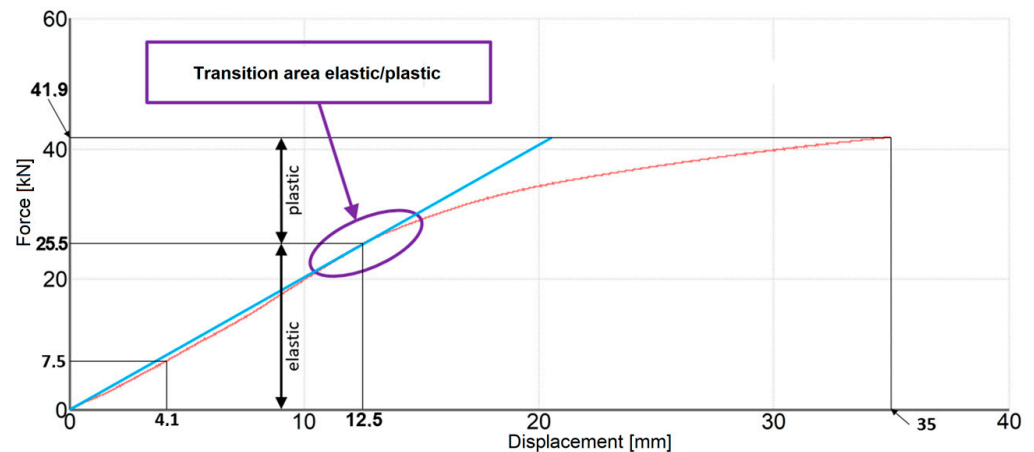
Figure 15. Characteristic curve of the towing system.

For complex stresses, the ability of the tensile and compressive strength testing machine is to strictly record the actuation force values and the linear deformation in the direction of actuation of the force and, based on these two properties, it generates a force–displacement diagram.

With the fixture attached to the platen of the tensile testing machine and the towing system secured to the fixture (Figure 16), settings were made on the machine for slow-speed application of the load on the towing assembly. This setting is necessary to be able to quickly detect any excessive horizontal movements of the towing hook (with the risk of the ball slipping outside the force actuation punch), to stop the test process immediately.
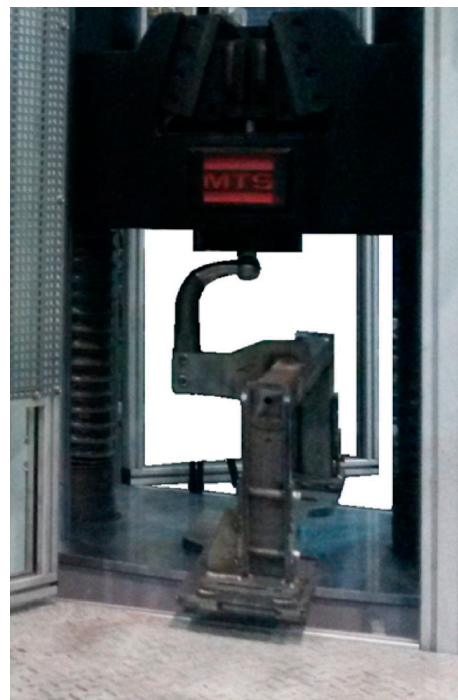

Figure 16. The towing system attached to the tensile testing machine.

The experiment had to be stopped because the hook had bent substantially so that the stress element of the test machine was acting almost on the neck and the bent area of the tow hook, and testing would have continued with results irrelevant to the study.

In this type of experimental test, the area where the greatest effort occurs can only be determined by analogy to the theoretical research of analytical and (or) numerical calculation. In the research on the classical resistance calculation, but also from the FEM,

it was found that in the towing hook, in the inner area of the radius of curvature, the highest tension occurred in the entire towing system. Therefore, in the experimental study of the towing system, it will be considered that the highest stress also occurs in the area of the hook indicated above, and with the values of the forces recorded by the strength testing machine, the calculation of the stress appearing in the towing hook will be achieved (Figure 15).

Table 4 shows the values of the forces measured by the test machine, the displacements appearing in the system in the vertical direction (corresponding to the longitudinal axis of the vehicle), but also the results of the stresses in the hook, corresponding to the forces in the elastic and plastic domains, respectively. The determination of the stress in the towing hook was carried out by analogy with the FEM, since the classical calculation only considers the bending stress using the curved bar theory (Winkler), omitting the adjacent, otherwise very low, tensile and compressive stresses.

Table 4. Behavioral characteristics of the towing system.

Characteristic	Force [kN]	Stress [MPa]	Displacement [mm]
Analytical calculation area, necessary for the study	7.5	184.9	4.1
The limit of elasticity	25.5	628.7	12.5
The maximum acting force on the system	41.9	1.033	35

3.3. Experimental Determinations on Towbar

The load encountered in the experimental determination of the towing hooks is not pure, being a load composed of bending with traction–compression. For this reason, before the experimental determination of the stresses and deformations occurring in the towing hooks, experimental tests were carried out on the specimens, both in tension and in bending.

The main stress is bending and occurs along almost the entire length of the hook, from the neck area to the hole furthest from the ball.

Bending stress causes repercussions on the material, namely the following: compression throughout the volume of material inside the radius of curvature, from the surface to the middle of the fiber (denoted Compression 1 in Figure 17), and tension throughout the volume of material outside the radius of curvature, from the middle fiber to the surface (denoted Traction in Figure 17).
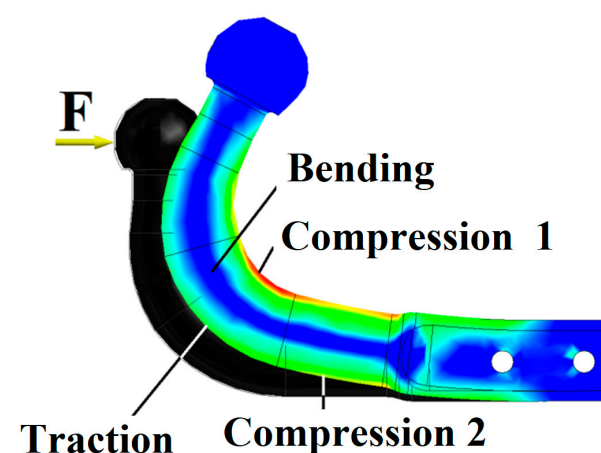

Figure 17. Forces appearing in the towing hook.

The compressive stress denoted by the phrase "Compression 2" in Figure 17 occurs strictly due to the compressive force on the ball of the towing hook, this stress being on the

entire volume of material starting from the curved area to the hole closest to the sphere. This loading causes the volume of material inside the middle fiber (toward the inside of the radius of curvature) to have a higher stress than on the outside, where a tensile stress occurs; "Compression 2" and "Tension" are stresses of opposite directions. This is one of the reasons why the higher stress is inside of the radius of curvature, with confirmation also received from the finite element analysis and also from the analytical calculations of the stress appearing in the towing systems used in motor vehicles.

The behavior of the tested towbars differs greatly depending on the material from which each individual part is made, from different mechanical strengths to different modes of deformation or breaking.

The behavior of the carbon fiber towbar is linear and the force–displacement diagram in Figure 18 (experimentally drawn by the author) confirms this. From the graph, it can be seen that there are two drops in force, which signifies the partial and inconstant destruction of the towbar's integrity.
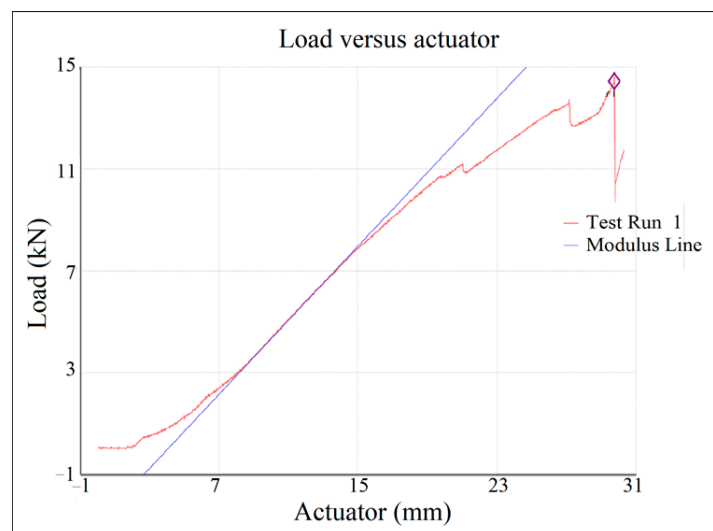

Figure 18. Characteristic curve of the carbon fiber towbar.

Another positive aspect of the carbon fiber composite is that it did not disintegrate in the area of adhesion between the carbon fibers and the metal sphere.

This hook has a disadvantage in behavior because in Figure 19 traces of total disintegration are observed in the area of its tail (macrocracks when flattening), but the positive aspect of this inconvenience is that the hook did not completely break into several parts, as happened with the equivalent tested specimens. If the pressing force of the traction machine had continued to act on the hook, it would certainly have suffered breakage into several components, but the displacement of the ball was quite pronounced, and the punch no longer acted on the sphere, but in the neck area, where traces of contact are observed; therefore, the testing process was interrupted.

Another argument for stopping force on the towbar was that there was a sudden drop in force on the chart, a sign of considerable disintegration of the tested element. The carbon fiber towbar broke in that area because the steel bushing, carbon fiber, and epoxy resin did not take the force as a homogeneous material and work together. Due to the stress, the bush broke the adhesion of the fibers and caused additional pressure on them, until some fragments of the composite material gave way.

The steel towbar had the most favorable force behavior in that it withstood the highest force and did not experience major damage or breakage either, only plastically deforming, as shown in the diagram in Figure 20.
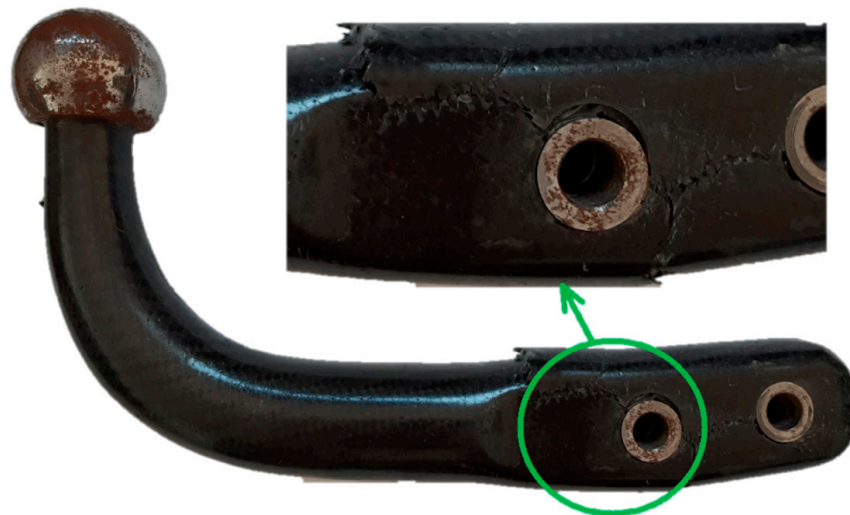
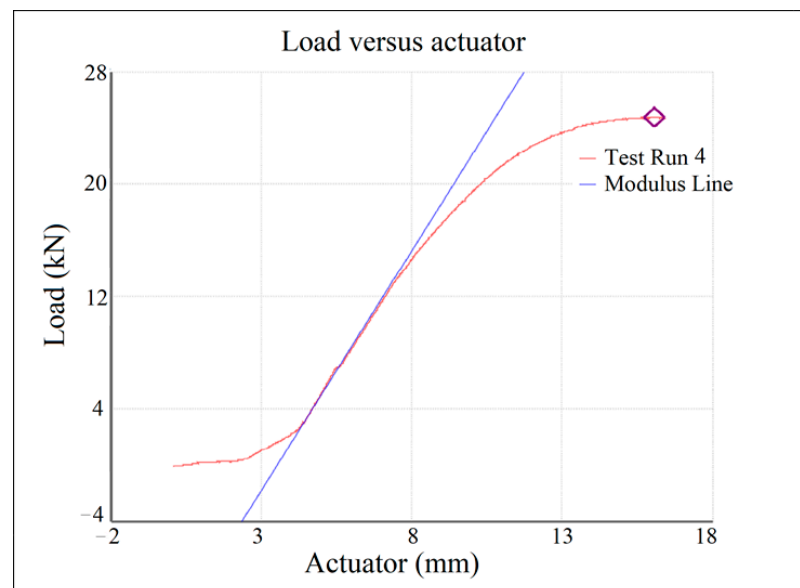**Figure 19.** Characteristic curve of the carbon fiber hook.

Figure 20. Characteristic curve of S355 steel hook.

Although the stroke of the traction machine acted under a load of 13.3 mm, and according to the characteristic curve (Figure 20) the hook passed into the plastic zone, after release from the load it returned to the initial state and no plastic deformations were recorded, as shown in the chart.

Regarding the towing hook made of pure aluminum, it can be said that it had an advantageous behavior, because the deformation was carried out plastically, but without breaking; the major disadvantage is the very low resistance.

The force–displacement diagram obtained from the traction machine (Figure 21) is atypical because a sudden increase in force is observed. If it were not for this force jump, it could be stated that this hook undergoes a constant, linear deformation throughout the testing process.
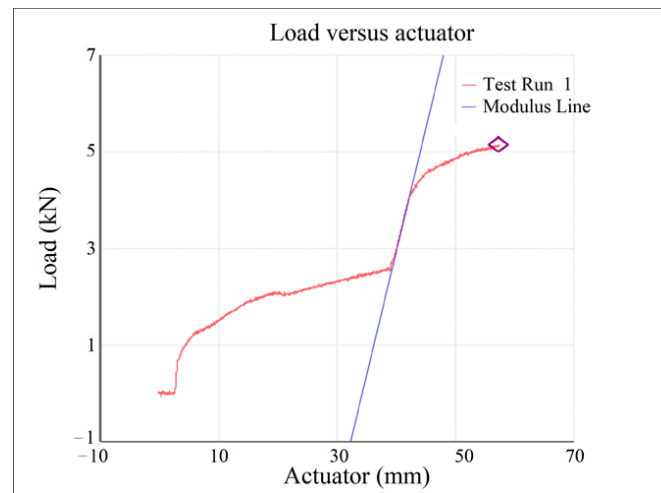
Figure 21. Characteristic curve of Al99.7% hook.

The reason this force jump occurs is that the ball of the hook moved a lot, released from the driving area of the punch of the testing machine, and the punch acted on the throat of the hook, thereby lowering the action arm of the force, increasing the downward force required to cause deformation.

Based on this consideration, the maximum force at which this towing hook would have been deformed would have been lower; therefore, in Figure 22, where all the curves are accumulated in one graph, its characteristic curve has been continued with a dotted line hook, resulting in a maximum force of 2.9 kN.

Figure 22. The Al99.7% hook, after testing.

Considering the real compressive force on the ball of the towing hook (theoretical force, less than that obtained on the traction machine), it can be said that the strength of the pure aluminum hook is around 12% of that of the steel hook, a difference which is considerably higher than in the case of the comparison of specimens subjected to bending (≈20%).

Figure 22 shows the plastic deformation suffered by the Al99.7% tow hook, deformation that did not disappear after the hook was released from the load; it did not return to its original shape, as happened with the steel hook.

Hooks made of AlSi10MnMg and AlSi12Cu1Fe have similar behavior, the characteristic curves resulting from the application of forces being curvilinear, as indicated by the diagrams in Figures 23 and 24.
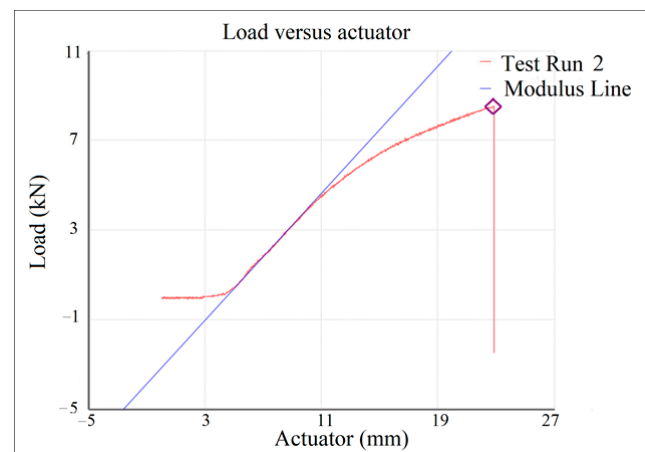
Figure 23. Characteristic curve of AlSi10MnMg hook.

Figure 24. Characteristic curve of AlSi12Cu1Fe hook.

The AlSi10MnMg alloy produces components with higher strength, but also with a higher elongation coefficient than AlSi12Cu1Fe components.

Another similarity between the results obtained from the experimental determinations is that both suffered breakage; moreover, this occurred in the same area (Figures 25 and 26), which is disadvantageous in the car manufacturing industry.

Figure 25. AlSi10MnMg tow hook, disintegrated.

Figure 26. AlSi12Cu1Fe tow hook, disintegrated.

Comparing the fracture areas of the two aluminum alloy tow hooks with Figure 17, which virtually shows the area with the most pronounced stresses, it is observed that there is similarity, but at the same time a confirmation based on experimental determinations is needed to show that the area indicated in the theory with the finite element method is correct and that it is the area where the greatest stress is encountered in the studied towing hook.

In Table 5, the results obtained from the experimental determinations are presented, adding the specific mass of the towing hooks, but also the force corresponding to each hook reaching the plastic domain, respectively, breaking. The maximum stress values in the table are obtained by analogy with the FEM.

The specimens that fractured under stress are of the same materials as the tow hooks that fractured in the test, namely, AlSi10MnMg and AlSi12Cu1Fe. From the testing of the samples, it was found that these materials are more brittle, presenting a poor elongation coefficient.

Even though it was not completely damaged (as can be seen with the hooks made of the two types of silumins), the integrity of the carbon fiber tow hook was considerably affected, with only a few connecting fibers remaining not completely destroyed. The same happened in the case of the specimens made of both types of composite materials when the fracture under the bending stress was almost complete, the two parts of the specimens being kept in contact by only a few fibers.

The towing hooks that did not break during the tests are of the same materials as the specimens that did not break under the bending stress, these materials being S355 steel and 99.7% Al. When testing the samples, it was found that these materials are more elastic, presenting a higher elongation coefficient.

The translation of some values from Table 5 into a force graph is shown in Figure 27, where it is observed that for the same design of hooks, with the same shape and the same sections, the highest strength is presented by the towing hook made of S355 steel, and the continuation of this chapter will present reports of the types of alternative materials to steel, steel being the material from which towing hooks are currently manufactured worldwide.

The characteristic curves, obtained as a result of experimental determinations, specific to the five towing hooks are superimposed in the diagram in Figure 28, and this image highlights very well their behavioral differences.

Analyzing the curves in Figure 28, it can be seen that the best hook is the one made of steel, followed by the one made of carbon fibers, and the worst is the one made of pure aluminum; those of alloys are superior to that of Al99.7%, but the advantages of each type of material are listed below, even if they present poor strength.
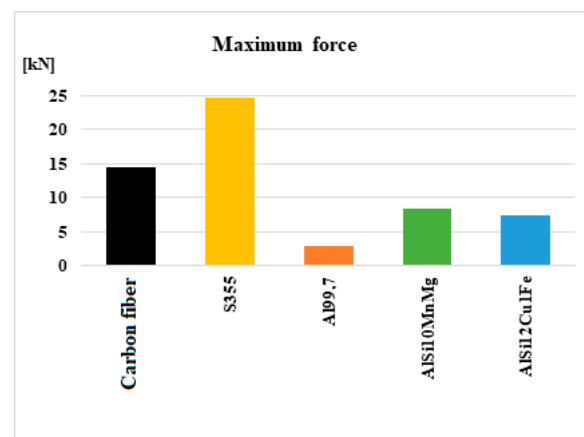
Figure 27. The maximum force applied to the towing hook.

Table 5. Experimental measurements of towbars.

Material	Maximum Force	Maximum Displacement [mm]	Maximum Stress [MPa]	Specific Mass [Kg/m³]	Rupture YES/NO
Carbon Fibers	14,436	27.65	354.36	780	YES and NO **
Steel S355	24,724	13.85	606.89	3.400	NO
Aluminum Al99.7	5134 *** 2905	54.60	71.31	1.050	NO
AlSi10MnMg	8504	18.80	208.74	1.050	YES
AlSi12Cu1Fe	7401	15.40	181.67	1.050	YES

In the frame that highlights the specific mass, it should be remembered that both the ball and the bushings near the fixing holes of the carbon fiber towing hook are made of steel, components that considerably increase its mass. ** In the border showing the final state of the towbars (after applying the breaking force), for the towbar made of carbon fiber and epoxy resin, there is the dual information that the product broke and did not break. This paradox arises because the tow hook did not break in the critical area where it was expected to, where the maximum stress resulting from the theoretical calculations occurs, nor in the bonding area between the fibers and the steel ball. It broke in the area of the metal pin located in the part closest to the ball, in the part farthest from the force actuation axis. The mounting holes are tension concentrators (Figure 19). *** In the frame where the maximum force acting on the ball of the towbar made of pure aluminum is highlighted, two forces are noted. The highest force of 5.134 kN appears on the diagram obtained from the test machine, but in the process of testing this hook there was an excessively large deformation, and for this reason the punch of the traction machine moved from the ball to the neck of the hook towing. From this moment, the evolution of the force was accentuated, but without relevance in this study; therefore, the continuation of the characteristic curve specific to this experiment was drawn with a dotted line (Figure 28).
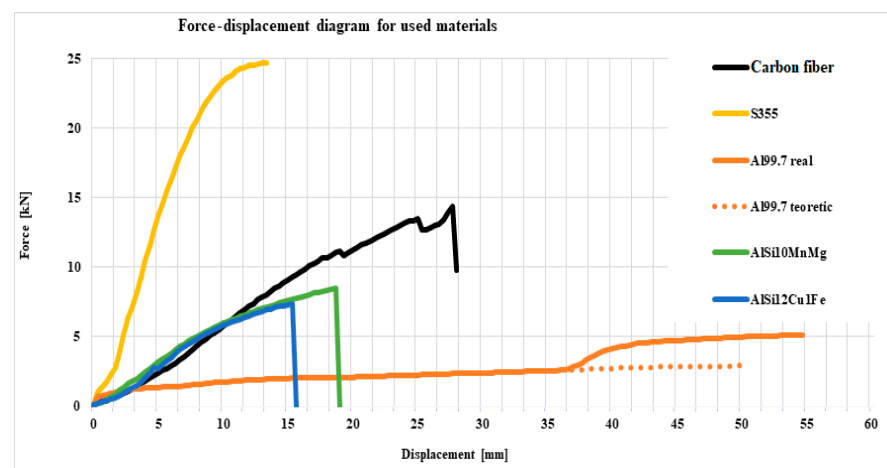

Figure 28. Superposition of the characteristic curves of the towing hooks.

Analyzing the two diagrams in Figures 27 and 28, as well as the values in Table 5, the following can be concluded (through multiple comparisons):

➢ The carbon fiber towing hook has up to 60% of the strength of the steel one, and the ball displacement is almost double, making it the strongest hook among the hooks made of alternative materials.

➢ The same carbon fiber hook shows two sudden decreases in strength, which signifies a state of inhomogeneity, either by the detachment of the metal bushings from the carbon fiber structure, or by the local destruction of some groups of carbon fibers; both possibilities are plausible because, according to the experimental determination, detachment of the two bushings from the fiber structure is observed, as well as ruptures of some groups of fibers.

➢ The AlSi10MnMg towbar has a strength below 35% that of steel, and the displacement is up to 35% higher, this hook having lower performance compared to the one made of carbon fibers, but higher performance compared to AlSi12Cu1Fe.

➢ The AlSi12Cu1Fe hook shows around 30% of the strength of the steel one, the displacement values of the two products being comparable.

➢ The hook made of Al99.7% is the most deficient in terms of mechanical strength, having a resistance of around 12% of that of the steel hook, but it has an excessively high displacement value, being 3.5 times higher.

Since, up to this point in the current chapter, references have been made only to the mechanical strength obtained by each individual towing hook, we believe that the analysis of their specific masses through the same diversity of materials should not be neglected. In this regard, the graph in Figure 29 shows the considerable differences in values between the materials chosen for this study.
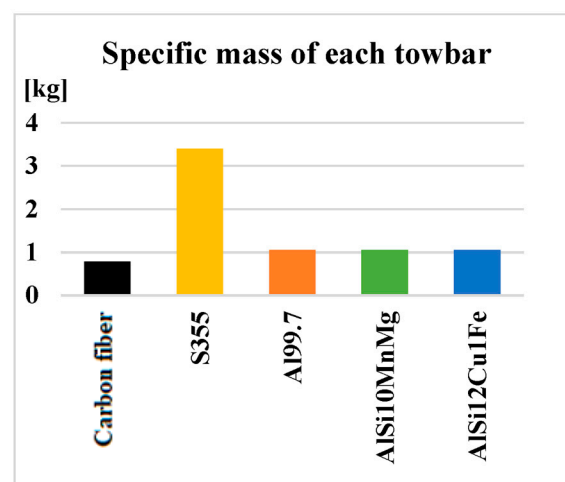

Figure 29. Performance of alternative material towbars.

This time, the highest values for the towing hooks do not represent advantages, as happened in the diagram where the mechanical strength was represented; on the contrary, they are disadvantages.

If from the point of view of mechanical properties the most advantageous hook is the steel one, in terms of specific mass it is the most disadvantageous. It weighs four times more than the carbon fiber tow bar and three times more than every tow bar made of aluminum or aluminum alloy. From the point of view of mass, the carbon fiber towbar is the most advantageous, but the aluminum and siluminum hooks are not without interest either. The aspect regarding the mass of the specimens is the first argument in the study of alternative materials as possible replacements for steel towbars.

If the value of the maximum force applied to the towing hook is related to its specific mass, for each individual specimen, comparison indices with a specific unit of measurement

$i_c = \frac{F}{m}$ are obtained. Through these comparison indices, the performance resulting from the ratio of the two analyzed properties of the studied materials is obtained. The obtained index values, but especially their comparative analysis, represent very important arguments in the continuation of this study regarding the identification of alternative materials in the construction of towing systems used for motor vehicles—Figure 30. The higher the index is, the more specifically the material of that index is performing.
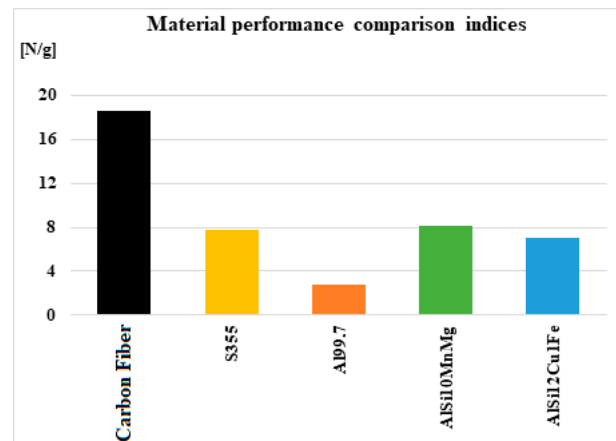

Figure 30. Performance comparison indices of alternative towbar materials.

Observing the dimensions of the indexes mentioned in Figure 30, it can be seen that the material with the most advantageous mechanical properties in terms of strength and mass is carbon fiber mixed with epoxy-type resin, the properties of this material categorically surpassing the properties of steel, but also those of aluminum and siluminium.

Comparing the obtained indices of the tow hooks made of siluminium and steel, it can be stated that they are comparable, the material AlSi10MnMg being slightly superior to steel, and AlSi12Cu1Fe slightly inferior. The index corresponding to the aluminum hook is clearly lower than all the other indices of the materials in the analysis.

Figure 31 shows the performance of alternative materials compared to the material used today in the construction industry for towing equipment—steel. The graph was plotted by relating the comparison indices of alternative materials with the steel index. Through this report, performance coefficients expressed in percentage are obtained, percentages with values above 100% signifying the overclassification of steel, and lower percentages representing materials with the mentioned properties inferior to those attributed to steel. Regarding the graph in Figure 32, which represents the performance of the materials, it can be said that it expresses a percentage interpretation of Figure 32, the one in which the comparison indexes of the performance of the materials studied in this paper are presented.
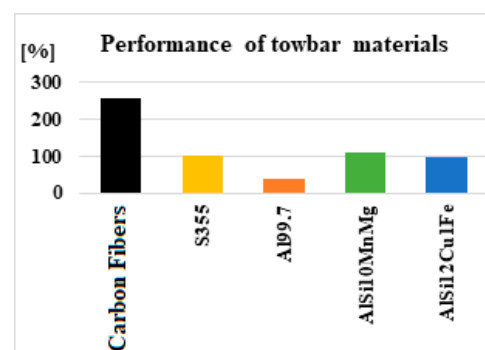

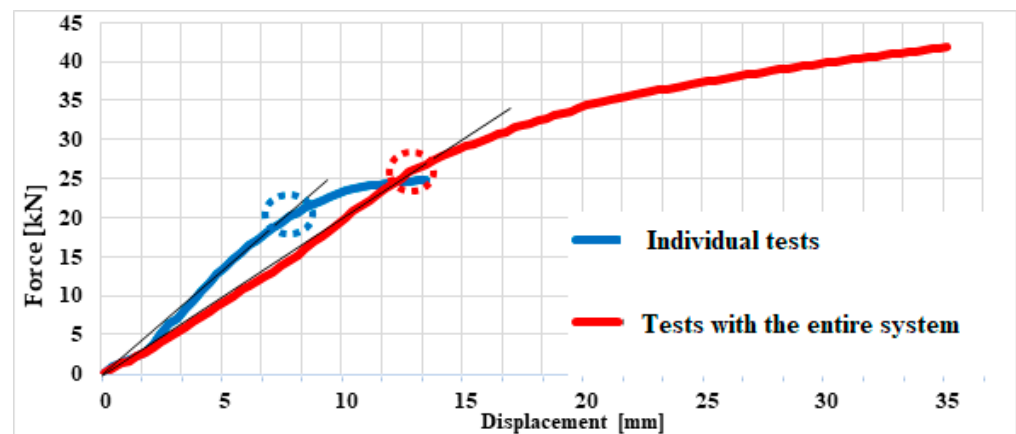**Figure 31.** Performance of towing hooks made of alternative materials.

Figure 32. Superposition of the characteristic curves of the steel towing hook and the towing system.

Analyzing Figure 31, it can be seen how the performance of the carbon fiber towbar is over than 250% of the performance of the steel one. In other words, the composite material based on carbon fiber and epoxy resin is 2.5 times more efficient than steel.

The AlSi10MnMg towbar is around 11% more efficient, the AlSi12Cu1Fe alloy is around 3% less efficient, and the pure aluminum hook has the lowest performance, around 38% of the steel one.

The interpretation of the two graphs in Figures 30 and 31 can be carried out in another, rather complex way, as follows:

If towing hooks were produced from the same types of alternative materials studied and if the design of these hooks from the alternative materials was changed, in the sense of scaling the model, they would have masses equal to that of steel (3.4 kg) and the following conclusions could be drawn:

➢ The towing hook made of composite materials based on carbon fibers would have a mechanical strength superior to that of steel, approximately 2.5 times higher;
➢ Aluminum alloy towbars would have similar mechanical strengths to steel, AlSi10MnMg slightly higher (by around 11%), and AlSi12Cu1Fe slightly lower (by around 3%);
➢ The pure aluminum towbar would have a significantly lower mechanical strength than steel (around 38% of its strength);
➢ A disadvantage of the towing hooks made of the two types of aluminum alloys is the fact that, following the gradual application of force, they reached the stage of being completely destroyed ending up forming two independent bodies.

The automotive industry is restrictive in this sense, requiring that in the event of an accident or a shock to a vehicle, there are no components that detach; the concept of "no flying parts" exists. It would be an unpleasant situation if, in the event of braking during a turn, the trailer continued its movement in the opposite direction, being independent of the turn of the vehicle. To compensate for this inconvenience, improving the elasticity of the alloy could be studied, by alloying with various other chemical elements, thus obtaining a hybrid material that is not as fragile.

4. Discussion

By comparing the behavior of the steel towing hook tested individually with the behavior of the towing hook tested in the towing assembly, some extremely interesting phenomena encountered in the two experimental test processes can be presented. When superimposing the characteristic curves specific to the towing system and the individual towing hook in Figure 32, considerable variations in the strength of the main debated component are observed. Looking at material entering the plastic field, Figure 32 shows the following:

- The individually tested towing hook reaches the plastic domain at an approximate force of $F_I = 21$ kN;

- The tested towbar as a whole reaches the plastic domain at an approximate force of $F_A = 25.5$ kN.

Taking into account the two findings above, it follows that a greater force is required to deform the towbar as a whole, F_A, than the force required to deform the individual tow hook—F_I.

$$F_I < F_A, \tag{1}$$

By hypothesis, it is considered that the elastic limit tension of the hook is the same, regardless of the test method, either individually, σ_{eI}, or as a whole—σ_{eA}.

$$\sigma_{eI} = \sigma_{eA} \tag{2}$$

By analogy with relation (1) and unfolding relation (2), we obtain the following:

$$\sigma_{eI} = F_I \cdot B_{FI}; \ \sigma_{eA} = F_A \cdot B_{FA} \tag{3}$$

From which it follows that

$$B_{FI} > B_{FA} \tag{4}$$

The result of relation (4) is seen in Figure 33. This is due to the sliding of the ball of the hook, tending to increase the arm on which the force acts, thus resulting in less stress required to deform the tow hook.
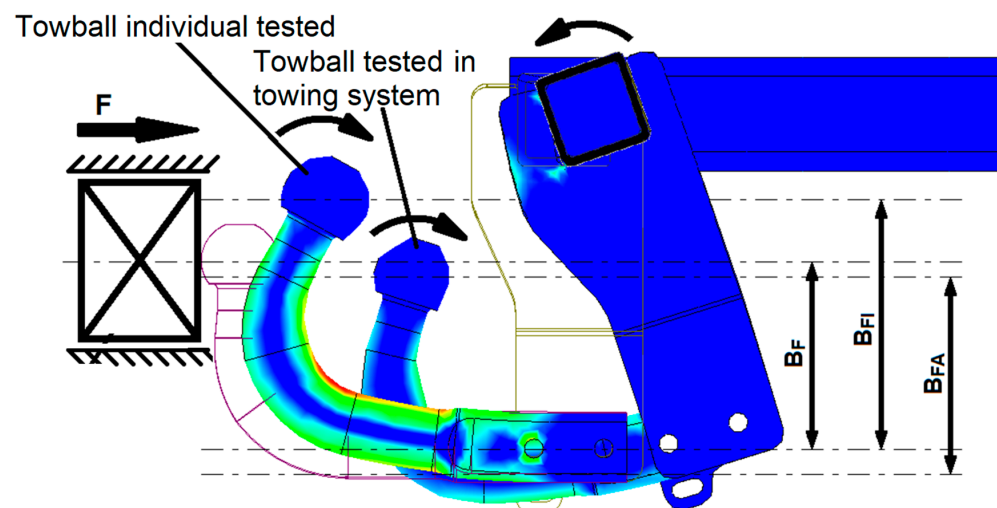

Figure 33. Superposition of the deformation mode of the tow hook tested individually and that tested in the tow assembly.

In the case of the tow hook tested in the tow assembly, the resistance beam tends to twist counter-clockwise, producing a stress against ball slippage; therefore, the whole tow assembly has a much more advantageous behavior than the individual product.

Regarding the deformations appearing in the system, analyzing Figure 33, the following conclusions can be drawn, considering the movement strictly in the direction of the driving force:

- Up to the force value F = 24.45 kN, the individually tested towing hook has a lower displacement than the one tested in the towing assembly. The deformation of the towing system is based not only on the deformation of the towing hook, but also on the deformations of the resistance beam and on the rotation of the central flanges.
- According to the force value F = 24.45 kN, the towing hook tested individually has a greater displacement than the one tested in the towing assembly. The deformation of the individually tested towbar increases excessively, while the force tends to increase very slowly, the product entering the plastic domain. The ball of the individually tested

towbar slides in the direction perpendicular to the direction of the force, increasing the force arm value. The towing assembly continues its linear motion because it has a few more units to travel before reaching the elastic limit.

- Around force F = 25.5 kN, the towing assembly reaches its yield strength, but the test process continues safely with integrity of the assembly. Near the value of F = 42 kN, the experimental testing stopped because the hook was rapidly deformed, the actuation punch being very close to contact with the bending area of the hook, which would have been followed by a considerable but irrelevant increase in force for the present study.

To fix the towing system, but also to fix the towing hooks on the tensile strength testing machine with a maximum force of 100 tons, specially made devices are needed, and the force acting on the system and on the hooks is gradually increased up to breaking or their significant deformation.

Being an assembly with complex geometries, for the towing system the deformation method and the distribution of internal stresses cannot be accurately known. Only after a preliminary analysis with theoretical determination methods can a potential deformation mode and potential critical areas be established.

Regarding the testing of the entire towing system, following theoretical analyses based on Strength of Materials calculations, but also with the help of the FEM, it is concluded that the highest stress in the system occurs inside the radius of curvature of the towing hook; therefore, in the experiment, emphasis is placed on the state of tension and deformation that occurs in the mentioned area.

The following stresses that occur in the structure of the towbar are complex: bending along the entire length of the towbar from the ball to the farthest hook fixing hole and compression and tension due to bending and compression.

Presenting the current situation, where the tow hooks are of similar design, it can be said that the steel tow hook has the highest mechanical strength, the carbon fiber tow hook is stronger than those made of siluminum, and the hook made of pure aluminum presents the weakest mechanical characteristics regarding strength.

On the other hand, regarding the situation in terms of the specific mass of each type of towing hook, it can be said that the most disadvantageous hook is the one made of steel, and the product with the lowest mass is the one made of carbon fibers. Aluminum and silumin hooks have a mass closer to that of a carbon fiber hook and very far from that of a steel hook.

By relating each of the values of the actuation forces on the hooks to the values corresponding to the specific masses of each hook, a comparison index is obtained. Higher index values represent higher performance for the hook made of that material. From this point of view, the best performing hook is by far the carbon fiber hook; the silumin hooks have similar performance to the steel one (AlSi10MnMg performing slightly better, AlSi12Cu1Fe performing less well) and the Al99.7% hook very poor performance.

Regarding the physical appearance of the hooks after testing, disregarding the actuation forces, it can be said that the products made of pure steel and aluminum are the most advantageous because they did not break, they only deformed plastically. The carbon fiber towbar did not break into multiple components, but it was completely damaged, breaking the bond between the metal inserts and the carbon fibers. The aluminum alloy components are also at a disadvantage in this regard because they broke, forming two parts independent of each other, and the automotive industry does not allow this type of behavior.

In order to reduce the discomfort created by the breaking of the towing hooks in the silumin, studies could be carried out to alloy with other chemical elements to decrease the property of the material being brittle.

One way to increase the mechanical strength of towing hooks is to optimize the constructive form of the semi-finished section. Also, by modifying this section, mechanical characteristics much inferior to the current solution can be obtained; therefore, the opti-

mization must be carried out thoroughly, studying the distribution of the stresses appearing in the system.

Improving the mechanical properties of aluminum alloy towbars can be achieved by applying an annealing heat treatment. In this way, the internal stresses in the material structure are eliminated (during the solidification phase).

Table 6 compares the results obtained with FEM calculation and classical calculation from the Strength of Materials.

Table 6. Critical stresses obtained by the 2 methods.

Method	Determination Area		
	The Inside of the Radius of Curvature of the Towing Hook, σ_{int}	The Outside of the Radius of Curvature of the Towing Hook, σ_{ext}	The Ends of the Resistance Beam of the Entire Towing System
	[MPa]	[MPa]	[MPa]
Classical model	188	117.04	63.82
FEM	184.9	118.6	63.4

Comparing the results obtained by the classic stress determination method and the finite element method, a very close similarity of the values is found, which is why the two methods are considered to be mutually validating. It is observed that the maximum stress values are approximately 50% of the elastic limit value ($\sigma_e = 355$ MPa) of the material from which the towing system is made; therefore, the technical solution presents a safety factor of 2. The system is neither undersized nor oversized, being considered a reliable system to the manufacturer's requirement.

Also, the obtained results indicate that the most stressed element in the entire towing assembly is the towing hook and with high results, but much lower than those in the hook, is the resistance beam.

The following improvement actions are possible:

- Since the carbon fiber towing hook suffered cracks in the area of the fixing bolts, it is proposed to optimize the shape of the tail of the hook to obtain an adequate strength.
- The manufacturing process of the carbon fiber towbar is laborious. An optimization involves a design change to help make the manufacturing process easier.
- Aluminum alloys hooks can undergo geometric changes to improve mechanical strength, since the casting process is more convenient than the technological flow of obtaining steel towing hooks.
- Also, the molding process in the forming mixture is very difficult; therefore, a pressure injection mold is proposed, both to optimize the molding process and to obtain a more compact structure of the material of the towing hooks made of aluminum.
- In order to improve the characteristics given by the strength of the aluminum towing hooks, studies are proposed regarding alloying with various other materials that offer higher resistance (e.g., Cu), as well as tests regarding the thermic treatment of the material from which the model is made.
- As a future development of this research, after establishing the processing procedures and choosing the most suitable materials for the construction of the towing hooks, it is proposed to expand the study of the reduction in the mass of the other components in the towing assembly by using alternative materials.
- It is necessary to carry out a study on dynamic fatigue tests of the towing system of alternative materials and on dynamic shock loads, especially if homologation of the system is expected.

5. Conclusions

By far the best strength was shown by the steel towbar, but the carbon-fiber-reinforced polymer (CFRP) towbar performed very advantageously, with a breaking force almost double that required for product validation.

The aluminum alloys (AAl) towbars were very close to the validation limit, with the AlSi10MnMg passing the test by easily exceeding the required force, the other performing slightly worse, but being very close to the limit.

In terms of sphere displacements, the most advantageous behavior was shown by the steel hook, with the smallest displacement, with the CFRP towing hook having the largest displacement.

The unsatisfactory characteristic features presented by the AAl towing hooks are due to the reduced plasticity, the material being very fragile, and breaking occurs suddenly.

When the strength of the hook is related to its mass (in the case of the same material), material performance indices are obtained, showing that the CFRP model is 2.5 times more efficient than S355, AlSi10MnMg 11% more efficient, and AlSi12Cu1Fe 3% below the performance of steel. These values provide guidance to researchers in the field of alternative materials for making tow hooks. Certainly, if CFRPs were improved, and also AAl, in order to obtain more homogeneous models, even higher performances would be obtained compared to those of steel.

There are several ways to obtain more advantageous results for AAl components, either through thermal treatments, in which recrystallizations will be obtained in the structure of the material to improve the plasticity properties, so that they are no longer as brittle and show superior strength, or by reducing the silicon content for better plasticity. On the other hand, silicon helps the metal bath to be more fluid, which is why the level of the chemical composition of the alloy should not be lowered too much. Annealing thermal treatments in order to eliminate internal stresses in aluminum-based structures, stresses resulting from solidification after the casting process, can considerably improve the mechanical properties of aluminum alloy or pure aluminum components.

Comparing the behavior of the steel towbar tested individually with that tested in the towing system as a whole, an interesting thing is observed. Twisting the strength beam of the tow assembly facilitates and helps the tow hook to suffer a lower sag.

By comparing the chemical composition of the two types of aluminum alloys, but especially the admissible field of tolerances for each alloying element, it is observed that the AlSi10MnMg brand alloy is more restrictive, having admissible limits in a very low tolerance field. For this reason, the development of the AlSi10MnMg alloy involves certain additional costs, primarily due to the need to use a larger amount of pure aluminum as a raw material.

The AlSi12Cu1Fe alloy has a more generous element tolerance; therefore, its elaboration is mainly carried out from waste of other alloy brands, which is why the manufacturing costs are lower than those for the elaboration of the AlSi10MnMg alloy. The latter is commercially available at a higher price than AlSi12Cu1Fe, but offers more advantageous properties.

In conclusion, this paper justifies the use of alternative materials in the automotive industry, due to the benefits regarding the costs and recycling of the materials used. The obtained results also explain the trend in this industry, oriented towards the replacement of steel with new and composite materials; at the moment, more than 50% of the components of a car are made of these materials, due to the advantages offered.

References

1. Czerwinski, F. Current Trends in Automotive Lightweighting Strategies and Materials. *Materials* **2021**, *14*, 6631. [CrossRef] [PubMed]
2. Chauhan, V.; Kärki, T.; Varis, J. Review of natural fiber-reinforced engineering plastic composites, their applications in the transportation sector and processing techniques. *J. Thermoplast. Compos. Mater.* **2022**, *35*, 1169–1209. [CrossRef]
3. Baker, A.A.; Scott, M.L. *Composite Materials for Aircraft Structures*, 3rd ed.; American Institute of Aeronautics & Ast.: Reston, VA, USA, 2016.
4. Barbero, E.J. *Introduction to Composite Materials Design*; CRC Press: Boca Raton, FL, USA, 2017.
5. Jarali, O.; Logesh, K.; Hariharasakthisudhan, P. Vibration Based Delamination Detection in Fiber Metal Laminates Composite Beam. *Rom. J. Acoust. Vib.* **2023**, *20*, 48–58. [CrossRef]
6. Usera, D.; Alfieri, V.; Ares, E. Redesign and manufacturing of a metal towing hook via laser additive manufacturing with powder bed. *Procedia Manuf.* **2017**, *13*, 825–832. [CrossRef]
7. Polasik, J.; Walus, K.J.; Mielniczuk, J. Experimental study of the tilt angle body of towing vehicle with different load. In Proceedings of the 21st Polish-Slovak International Scientific Conference on Machine Modeling and Simulations (MMS2016), Hucisko, Poland, 6–8 September 2016; Volume 177, pp. 271–274.
8. Zatocilová, A.; Koutny, D.; Brandejs, J. Experimental Verification of Deformation Behavior of Towing Hitch by Optical Measurement Method. In *Modern Methods of Construction Design: Proceedings of ICMD 2013*; Springer: Cham, Switzerland, 2014; pp. 420–430.
9. Narayanan, S.V.S.; Peters, D. Design and Control of Vehicle Trailer with Onboard Power Supply. *SAE Int. J. Passeng. Cars-Electron. Electr. Syst.* **2015**, *8*, 32–40. [CrossRef]
10. Dehadrai, A.R.; Sharma, I.; Gupta, S.S. Three-Dimensional Dynamics of Towed Underslung Systems Using Geometrically Exact Beam Theory. *AIAA J.* **2021**, *59*, 1469–1482. [CrossRef]
11. Eisenmann, J.; Horsley, J.; Peters, D.L. Small-Scale Physical Modeling and Testing of a Vehicle Trailer with Onboard Power Supply. In Proceedings of the ASME International Design Engineering Technical Conferences and Computers and Information in Engineering Conference (IDETC/CIE), Charlotte, NC, USA, 21–24 August 2016; Volume 2A.
12. Petracconi, C.L.; Ferreira, S.E.; Palma, E.S. Fatigue life simulation of a rear tow hook assembly of a passenger car. *Eng. Fail. Anal.* **2010**, *17*, 455–463. [CrossRef]
13. Trotea, M.; Constantinescu, A.; Simniceanu, L. Design Optimization of the Towing Hook Used in Passenger Cars for Light Trailers. In Proceedings of the 30th SIAR International Congress of Science and Management of Automotive and Transportation Engineering (SMAT), Jessup, MD, USA, 27 July–7 August 2020; pp. 540–549.
14. Wang, Z.P. Car Front Towing Hook Analysis and Structural Improvements Based on CAE. In Proceedings of the 2015 International Industrial Informatics and Computer Engineering Conference, Xi'an, China, 10–11 January 2015; pp. 1113–1116.
15. Balcau, M. Aerodynamic Study of a Car Towing a Motocycle Trailer. *Ing. Automob.* **2021**, *58*, 22–26.
16. Hands, S.J.; Zdravkovich, M.M. Drag Reduction for a Passenger Car Towing a Caravan. *J. Wins Eng. Ind. Aerodyn.* **1981**, *9*, 137–143. [CrossRef]
17. Lufinka, A. Crash test of a tow hitch for car trailers. In Proceedings of the 57th International Scientific Conference on Experimental Stress Analysis (EAN 2019), Luhacovice, Czech Republic, 3–6 June 2019; pp. 264–268.
18. Teodorescu-Draghicescu, H.; Vlase, S.; Scutaru, M.L.; Serbina, L.; Calin, M.R. Hysteresis effect in a three-phase polymer matrix composite subjected to static cyclic loadings. *Optoelectron. Adv. Mater.-Rapid Commun.* **2011**, *5*, 273–277.
19. Lee, S.W.; Chung, P.W. *Finite Element Method for Solids and Structures: A Concise Approach*; Cambridge University Press: Cambridge, UK, 2021.
20. Katouzian, M.; Vlase, S.; Scutaru, M.L. Finite Element Method-Based Simulation Creep Behavior of Viscoelastic Carbon-Fiber Composite. *Polymers* **2021**, *13*, 1017. [CrossRef] [PubMed]
21. Su, R.H.; Wang, B.J.; Peng, C.Y. The finite element analysis on driving wheel-axle system of adhesive tape conveyor with steel wire towing. In Proceedings of the 3rd International Symposium on Modern Mining and Safety Technology, Fuxin, China, 4–6 August 2008; pp. 833–837.
22. Dizo, J.; Blatnicky, M.; Kafrik, A. Investigation of Driving Stability of a Vehicle-Trailer Combination Depending on the Load's Position Within the Trailer. *Acta Mech. Autom.* **2023**, *17*, 60–67.

23. Mioch, T.; Kroon, L.; Neerincx, M.A. Driver Readiness Model for Regulating the Transfer from Automation to Human Control. In Proceedings of the 22nd International Conference on Intelligent User Interfaces (IUI-2017), Limassol, Cyprus, 13–16 March 2017; pp. 205–213.

24. Barbosa, R.M.; Medeiros, E.B. Evaluation of Dynamic Characteristic of Structural Panels with Statistical Energy Analysis. *Rom. J. Acoust. Vib.* **2023**, *20*, 139–146.

25. Li, T.; Zhang, N.; Ma, J.; Yin, G.D. Stability Investigation of Car-trailer Combinations considering Steering System Stiffnesstr. In Proceedings of the 31st Chinese Control and Decision Conference (CCDC), Nanchang, China, 3–5 June 2019; pp. 6040–6045.

26. Codarcea-Munteanu, L.; Marin, M.; Vlase, S. The study of vibrations in the context of porous micropolar media thermoelasticity and the absence of energy dissipation. *J. Comput. Appl. Mech.* **2023**, *54*, 437–454.

27. Zhang, N.; Yin, G.D.; Chen, N. Analysis of Dynamic Stability of Car-trailer Combinations with Nonlinear Damper Properties. In Proceedings of the IUTAM Symposium on Nonlinear and Delayed Dynamics of Mechatronic Systems, Nanjing, China, 17–21 October 2017; Volume 22, pp. 251–258.

28. Vörös, I.; Takács, D. The Effectes of Trailer Towing on the Dynamics of a Lane-Keeping Controller. In Proceedings of the Annual ASME Dynamic Systems and Control Conference (DSCC2020), Pittsburgh, PA, USA, 5–7 October 2020; Volume 1.

29. Khalkar, V.; Hariharasakthisudhan, P.; Kalamkar, R. Some Studies Verify the Applicability of the Free Vibration Method of Crack Detection in Composite Beams for Different Crack Geometries. *Rom. J. Acoust. Vib.* **2023**, *20*, 30–41.

30. Borsutkar, S.; Gujar, A.; Dongarkar, Z.; Chavan, V.; Horambe, P. Design and Fabrication of Car Towing Attachment. *Int. J. Adv. Res. Sci. Commun. Technol.* **2024**, *4*, 309–312. [CrossRef]

31. Abouelregal, A.E.; Marin, M.; Öchsner, A. The influence of a non-local Moore–Gibson–Thompson heat transfer model on an underlying thermoelastic material under the model of memory-dependent derivatives. *Contin. Mech. Thermodyn.* **2023**, *35*, 545–562. [CrossRef]

32. Marin, M.; Öchsner, A.; Vlase, S.; Grigorescu, D.O.; Tuns, I. Some results on eigenvalue problems in the theory of piezoelectric porous dipolar bodies. *Contin. Mech. Thermodyn.* **2023**, *35*, 1969–1979. [CrossRef]

33. Saputro, R.K.; Afisa, T.; Hendratno, D.S.P.; Reginawati, T.; Hilal, A.; Ambarwati, D. *Innov. Bus. Manag. Account. J.* **2023**, *2*, 67–76. [CrossRef]

34. Caruso, M.; Gorella, N.S.; Gallina, P.; Seriani, S. Towing an Object with a Rover. *J. Mech. Robot.* **2024**, *17*, 021001. [CrossRef]

35. Zhao, L.J.; Yang, J.G.; Jiang, J.H. Testing the Hybrid Hydraulic Drive Aircraft Tractor Via LXI Bus Technique. In Proceedings of the 2009 International Workshop Information Security and Application, Busan, Republic of Korea, 25–27 August 2009; pp. 47–50.

36. Wang, N.J.; Liu, H.B.; Yang, W.H. Simulation Study of the Backward-Motion for a Aircraft Towbar less Tractor. In Proceedings of the 12th IEEE International Conference on Computer-Aided Industrial Design and Conceptual Design, Chongqing, China, 1–8 January 2011; Volume 1–2, pp. 762–766.

37. Vlase, S.; Marin, M.; Bratu, P.; Bratu, P.; Manea, R.; Shrrat, O.A.O. Analysis of Vibration Suppression in Multi-Degrees of Freedom Systems. *Rom. J. Accoustic Vib.* **2022**, *19*, 149–156.

38. Olesen, A.V.; Elvik, R.; Lahrmann, H.S. Does a tow-bar increase the risk of neck injury in rear-end collisions? *J. Saf. Res.* **2018**, *65*, 59–65. [CrossRef] [PubMed]

39. Beregi, S.; Takács, D.; Barton, D.A.W. Stability analysis of the car-trailer system with a time-delayed tyre model. In Proceedings of the 24th Symposium of the International-Association-for-Vehicle-System-Dynamics (IAVSD), Dynamics of Vehicles on Roads and Tracks, Graz, Austria, 17–21 August 2015; pp. 643–652.

40. Park, M.; Chung, W.; Kim, M. Experimental research of a passive multiple trailer system for backward motion control. In Proceedings of the 2005-IEEE International Conference on Robotics and Automation (ICRA), Barcelona, Spain, 18–22 April 2015; Volumes 1–4, pp. 105–110.

41. Rükgaur, A.; Petersen, U.; Schiehlen, W. Lateral dynamics of towed vehicles. In Proceedings of the 2nd International Conference on Road Vehicle Automation (ROVA 95), Bolton, UK, 11–13 September 1995; Road Vehicle Automation II. pp. 90–99.

42. Szaksz, B.; Stepan, G. Delay Effects in the Dynamics of Human Controlled Towing of Vehicles. *J. Comput. Nonlinear Dyn.* **2023**, *18*, 061003. [CrossRef]

43. Modrea, A.; Vlase, S.; Horatiu, T.-D.; Mihalcica, M.; Calin, R.; Astalos, C. Properties of advanced new materials used in automotive engineering. *Optoelectron. Adv. Mater.-Rapid Commun.* **2013**, *7*, 452–455.

44. Semionovas, E.; Juodvalkis, D.; Skvireckas, R. The Stand Simulation of Stability of a Car with a Trailer. In Proceedings of the 22nd International Scientific Conference on Transport Means, Trakai, Lithuania, 3–5 October 2018; Volume PTS I-III, pp. 1265–1267.

45. Marin, M.; Chirila, A.; Oechsner, A.; Vlase, S. About finite energy solutions in thermoelasticity of micropolar bodies with voids. *Bound. Value Probl.* **2019**, *2019*, 89. [CrossRef]

46. Xavier, J.R.; Vinodhini, S.P.; Beryl, J.R. Innovative multifunctional nanocomposite coated aluminum alloy for improved mechanical, flame retardant, and corrosion resistance in automobile industries. *J. Adhes.* **2024**, *early access*.

47. Mokhtari, M.A.; Nikzad, M.H. Multi-objective optimization and comparison of machine learning algorithms for the prediction of tensile properties of aluminum-magnesium alloy. *Mater. Today Commun.* **2024**, *40*, 109476. [CrossRef]

48. Sun, Y.T.; Akçay, F.A.; Bai, Y.L. Analytical and numerical modeling on strengths of aluminum and magnesium micro-lattice structures fabricated via additive manufacturing. *Prog. Addit. Manuf.* **2024**, *early access*.

49. Gu, D.D.; Meiners, W.; Wissenbach, K.; Poprawe, R. Laser additive manufacturing of metallic components: Materials, processes and mechanisms. *Int. Mater. Rev.* **2012**, *57*, 133–164. [CrossRef]

50. Cui, J.R.; Roven, H.J. Recycling of automotive aluminum. *Trans. Nonferrous Met. Soc. China* **2010**, *20*, 2057–2063. [CrossRef]